Journal of Mechanical Engineering and Sciences (JMES)
ISSN (Print): 2289-4659; e-ISSN: 2231-8380
Volume 10, Issue 2, pp. 2076-2083, September 2016

DOI: https://doi.org/10.15282/jmes.10.2.2016.12.0196

Investigation on changes in gamma prime precipitate on varying surface locations of IN738 engine turbine blade

M. S. Hamizol[1], P. S. M. Megat-Yusoff[1, a], M. A. Nasrudin[1], M. A. Meor Said[1], M. S. Jasmani[2] and S.M.A. Syed Ahmad Ghazali[3]

[1]Mechanical Engineering Department, Universiti Teknologi PETRONAS,
32610 Bandar Seri Iskandar, Malaysia
[*]Email: puteris@petronas.com.my
[2]PETRONAS Upstream, Level 48, PETRONAS Tower 3, Kuala Lumpur City Centre
50088 Kuala Lumpur, Malaysia
[3]PETRONAS Carigali Sdn. Bhd., Peninsular Malaysia Operations,
Kompleks Operasi Petronas, 24300 Kertih, Kemaman, Terengganu, Malaysia

ABSTRACT

Changes in microstructure of a service exposed turbine engine blade have been found to affect the elemental composition and the performance because the existing bond structures, as well as the phase distribution of the blade material, deteriorates as a consequence of the changes. As such, this systematic internal deformation, which can expedite the creep and crack formation, has been a source of concern for the industry. Besides, failure in understanding these microstructural changes can lead to disregard of necessary and vital preventive measures. Hence, the present study investigates a turbine engine blade with estimated operating hours of 52000 at ±720^{o}C to examine the changes that occur in the microstructure of blade material from different points of the blade. For that purpose, scanning electron microscopy (SEM) was used to analyse the grain boundary formation and the gamma prime precipitates. In fact, the presence of the gamma prime phase in the microstructure had been proven to be a major contributing factor that enhanced nucleation and propagation creep. Other than that, the varied locations on the blade were examined and compared to determine the critical points that affected the performance of blade during operation using an electric discharge machine (EDM). Furthermore, the development of gamma prime precipitates had been rather obvious in the equilibrium phase than that in the solid phase due to temperature variation. On top of that, the transformation in the pressure surface location displayed more intensity than the suction surface location, in which limited carbides (MC) was observed in the suction surface location, whereas the grain boundary growth had been sporadic. However, continuous gamma prime precipitate was discovered in the pressure surface location. Hence, this study infers that changes that take place in the microstructure of the blade do not solely depend on the hours exposed or the intensity of subjected pressure, but such changes are deemed to occur due to a number of other essential aspects, for instance, material bulk properties, alloy constituents, loss of surface coherence, coarsening, and condition of operation.

Keywords: Microstructure; gamma prime precipitate; equilibrium phase; SEM; EDX

INTRODUCTION

Gas turbines are designed to operate under high temperature and pressure loading conditions. During such operations, the associated components go through some degradation phases due to changes in microstructure that can result in failure of mechanisms, such as corrosion, low and high cycle fatigue, and creep [1]. Creep significantly reduces the component life of stationary gas turbines. The major concern in designing turbine blades, nonetheless, is their ability to withstand creep deformation. Creep failure can occur below the yield strength of the material due to a constant applied load at elevated temperature condition and extended time [1]. Additional pressure condition also can accelerate the failure growth. Other than that, creep failures are hastened when the operating temperature condition reaches the melting temperature of the material; waning several mechanical properties, such as yield stress, creep lifetime, and low-cycle fatigue life[2]. Such deteriorations occur due to changes that take place in the mechanical properties of the material. Therefore, it is essential to acknowledge and comprehend the impact of temperature variation upon the microstructure of materials to hinder failure in material, particularly creep deformation failure[3]. The development of turbine blade is important due to its high demand in industries. Hence, this phenomenon has pushed researchers to further investigation and determine the influence of temperature on microstructure development and materials properties. For instance, low density and strong Topologically Close Packed (TCP) phase developed during exposure at elevated temperature generate low propensity that leads to grain defects[4]. Besides, nickel-based alloys are defined as nickels that contain varying alloying elements like refractory element, such as that found in molybdenum (Mo), tungsten (W), rhenium (Re), ruthenium (Ru), and tantalum (Ta) [5]. On the other hand, some define nickel-based alloys as those that mainly consist of carbides forming, γ^{I} forming, and refractory elements, such Mo, W, Ta, Cr (chromium), and Co (cobalt) [6].

Meanwhile, the nickel-based superalloy type functions as a combination of prominent high-heat creep-rupture strength and corrosion-resistant, which has been found to be better than many other high-strength superalloys with lower chromium content, for example Inconel 738 [7]. However, nickel alloy also possesses microstructure with multi-phases, such as gamma precipitate (γ) matrix, gamma prime precipitate ($\gamma^{I)}$ precipitates, carbides, as well as small amounts of deleterious phases, such liquid phase (δ), equilibrium phase (η), sigma phase (σ), and laves. Eventually, these phases determine the properties of the materials, besides influencing the performance and the lifespan of such alloy materials [8, 9]. The gamma prime γ^{I} phase occurs in three distinctive morphologies: eutectic lamellar γ^{I} formed between dendrite arms, primary cuboidal γ^{I}, and secondary spheroidal γ^{I} [10]. The γ^{I} phase is a super lattice that is comprised of the LI_2 type structure mainly composed of Ni_3 (Al, Ti). Meanwhile, the primary cuboidal (γ^{I}) is produced during solidification under 1200^{o}C, whereas the secondary spheroids γ^{I} is generated during aging after partial solution treatment. The secondary (γ^{I}) is smaller in size than that of primary γ^{I} by 0.7 μm[6]. Besides, coarsening and coalescence of γ^{I} precipitates can decrease the tensile strength in materials[10]. For example, investigations have revealed that the (γ^{I}) phase size grows when the operating condition of turbine engine is increased to approximately 1050°C[11]. In fact, the temperature that was increased from the normal operating condition had been 850°C. As such, interruption may occur in the cooling channel when the temperature elevates. Hence, understanding all aspects of the failure mechanisms would surely aid designers in the trade–off between different design options

and also help operators to make informed maintenance decisions. Moreover, the microstructure varies based on the respective zone or location. The creep strength is further reduced in the long term and it is subjected to the quality of heat treatment with austenitizing temperature. However, the difference of creep rupture strength is reduced in the long term region at around 40,000 h, whereas the decrease in creep rupture ductility of the forging hit 43,300 h[12]. Hence, owing to the peculiarity of the failure mechanics, an experimental investigation of microstructural profile of a service exposed IN738 turbine blade manufactured from Nickel super-alloy is investigated experimentally at varying locations of the blade at 720^{o}C for 52,000 hours.

EXPERIMENTAL DETAILS

Samples Preparation

First, a sample of the blade was cut and the chemical composition of the sample was determined via optical emission spectroscopy. Besides, in order to examine the microstructure of the blade, six samples were cut from different points of the blade to represent the suction and the pressure surface sides of the trailing edge inside the combustion chamber using an electric discharge machine (EDM). Figure 1 shows the cutting procedures and the locations of the metallographic specimen of various parts of the blade. Specimens (A_1, B_1, C_1) and (A_2, B_2, C_2) represent the pressure surface side and the suction surface side of the blade respectively. Besides, pre-treatments were carried out to enhance the quality of the sample specimen, as well as to capture the martensitic lath surfaces that contain high-density dislocations, coarsened laths with low-density dislocation, and cell-like sub-grain structures, which are found after creep rupture[12].

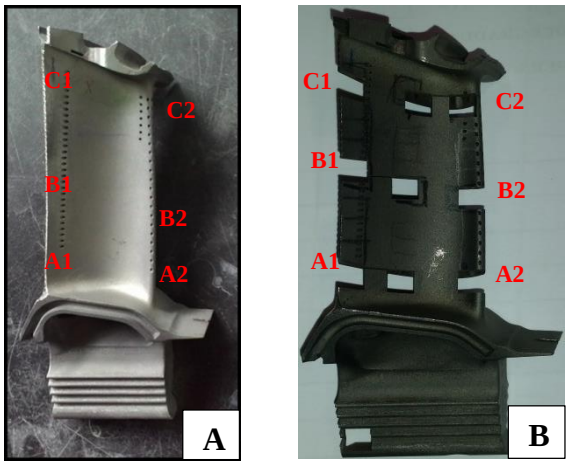

Figure 1. Turbine blade sample at different points (A) Before machining; (B) After machining.

Moving on to microstructural investigation, the microstructure of the samples was examined via optical microscopy after standard grinding and polishing procedures. Each sample was mounted using Buehler Simpliment 1000 automatic mounting presses, followed by grinding and polishing processes until a flat and mirror image surface was obtained. Later, the specimens were ground using Grit 240 up to 1200 silicon carbide papers and polished with 6 µm, followed by 1µm alumina with distilled water as suspension solution on low napped polishing cloth. Finally, the surface was etched to reveal the microstructure through selective chemical attack[13]. Here, the Kalling agent

was used, which comprised of 40 mL of ethanol, 40 mL of HCL, and 2 g of $CuCl_2$. The sample was immersed and swabbed for two to three minutes to reveal the microstructure. The chemical composition of IN738 [14] is summarised in Table 1.

Microscopy Observation

The microstructure of gamma prime (γ^I) precipitates phase was examined by using Zeiss SUPRA55VP with an accelerating voltage of 10kV on each sample point. The images were digitally recorded from a range of 1000x until 5000x magnification.

Table1. Chemical composition of IN738 superalloy.

Material	Composition (unit: wt. %)
IN 738	0.11C, 15.084Cr, 8.5Co, 2.48W, 1.88Mo, 0.07Fe, 0.92Nb, 3.46Al, 3.47Ti, 1.69Ta, 0.001S, 0.04Zr, 0.012B, balance Ni

RESULTS AND DISCUSSION

Each specimen from both the pressure side and the suction surface side locations had been examined by using SEM and comparison was made accordingly. Figure 2(a) illustrates the microstructure or the morphology observed at location A1. At this location, (γ^I) precipitates were observed as it was exposed to constant thermal and stress during the blade operation. The micrograph reveals over aging as the secondary structure of precipitates had been induced by these operating factors. The precipitates were nearly cubical, while some were spheroidal in shape. In fact, a similar conclusion was reported by [2], whereby the formation of grain boundary was mainly carbides. Other than that, the secondary spheroidal (γ^I) precipitates had been observed to vary in size and shape, which might be a result of exposure of the suction surface side to intense heat as the temperature rose. The grains boundary formation was intermittent. Furthermore, most of the secondary (γ^I) precipitates displayed a globular structure although some became coarser; resulting in a rougher edge or perimeter. This might be due to the prevailing elements, which is in agreement with a study by [15] that reported the dependency of (γI) precipitate phase in volume fraction upon Al or Ti contents. On top of that, a stone like structure can be observed at location A1, as highlighted by the arrows. These are the MC type carbides of seed like or stone structure that occur within the grain boundary, also as depicted in the literature [4, 15]. However, the structural shape of the MC carbides varied at various points on the surface. Similar results of these MC type carbides for IN738 turbine blade had been reported at different stages of the blade [6]. The MC carbides that had been observed were in the form of white structure due to the use of backscattered electron imaging (BEI) during SEM process. These precipitates could cause a reduction in the stress-rupture life, ductility, and micro hardness[10]. Besides, Figure 2(b) portrays the population of gamma prime (γ^I) precipitates in a vivid manner due to their bigger size and formation of joined structure compared to the population of gamma prime (γ^I) precipitates at location A1. In fact, bigger-sized secondary (γ^I) precipitates were observed at Location A1. Additionally, the distribution of the precipitates had been bimodal, in which the fine and primary (γ^I) precipitates were combined with huge-sized secondary (γ^I).

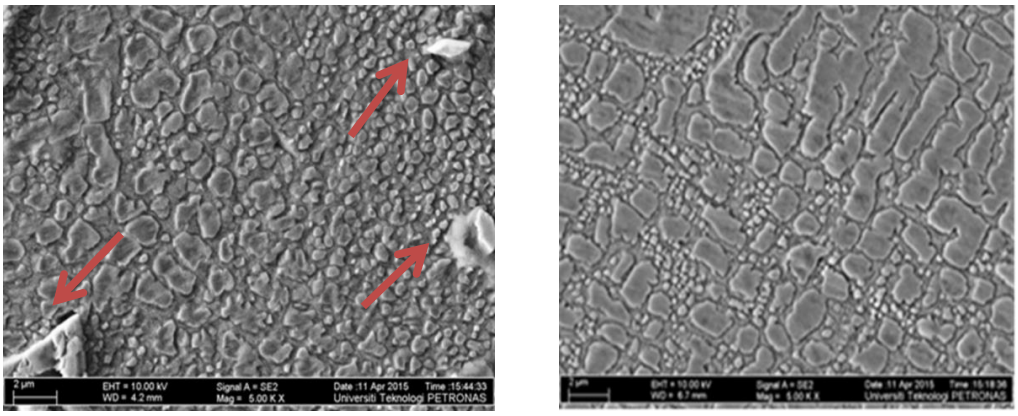

(a) (b)

Figure 2. (a) The microstructure at location A1; (b) The microstructure on location B2.

Moreover, the huge secondary (γ^I) precipitates were no longer in the form of globular and spheroidal. In fact, some of these secondary precipitates enjoined and formed elongated structures with rough edges. The primary gamma prime precipitates were dominant and well-formed; unlike the secondary gamma prime precipitates, as observed in the SEM imaging. Nevertheless, although discontinuous, these findings are in consonant with a study by [10], where the primary (cubical) (γ^I) were formed at the expense of the secondary (spheroidal) (γ^I) structure. Moreover, the formation of MC carbides had been more compared to that at location A1. Furthermore, the SEM micrograph at location C1, as shown in Figure 4, exhibits unexpected microstructure with defects. The defects or voids are reflected as dark spots in the microstructure. Hence, non-smooth surface was obtained for the turbine blade with the absence of (γ^I) population, which can cause potential environmental hazard due to the exposed surface. A similar observation reported by [9] on vicinity crack surface of IN738 showed that the population of (γI) precipitates disappeared along the crack paths.

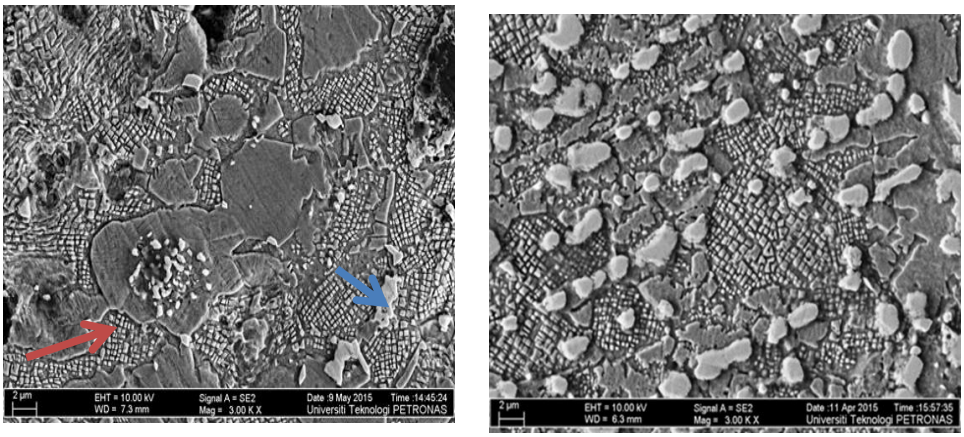

(a) (b)

Figure 3 (a) Microstructure on location C1; (b) Microstructure on location C2**.**

Figure 3(a) demonstrates two types of carbides formed at point C1. The formation of $M_{23}C_6$ was in the form of aligned carbide along the grain boundaries (bottom right of Figure 3(a)). Thus, the formation of $M_{23}C_6$ refers to the polycrystalline structure of the

material due to the existence of grain boundaries. However, the MC type carbides were smaller in six and randomly distributed without any specific orientation, as found in $M_{23}C_6$. In addition, MC carbides existed within grain boundaries; unlike $M_{23}C_6$[10]. Further observation of the microstructure revealed similar bimodal distribution of the (γ^I) precipitates. However, fine primary cuboidal (γ^I) precipitates developed into coarser and distinct cubical, as well as rectangular in shape. Meanwhile, the larger secondary (γ^I) precipitates evolved into bigger size than that observed at Locations A1 and B2. Meanwhile, the microstructure for location C1, as illustrated in Figure 3(b), displays the prominent existence of $M_{23}C_6$. $M_{23}C_6$ carbides were well organized in vertical and horizontal lines, which further indicates that the grain boundaries had been well oriented. However, the arrangement of $M_{23}C_6$ carbides started to distort due to a change in the arrangements of (γ^I) precipitates. As a matter of fact, this also indicates changes in the grain boundary. The background structure, nonetheless, still remained as bimodal (γ^I) precipitates. Meanwhile, the structure of secondary (γ^I) precipitates began to disappear and were replaced with primary (fine) (γ^I) precipitates. Hence, the distribution and the population of primary (γ^I) precipitates turned dominant. In fact, the structures of the primary (γ^I) precipitates developed into distinct cubical structure, as shown on Figure 3(b).

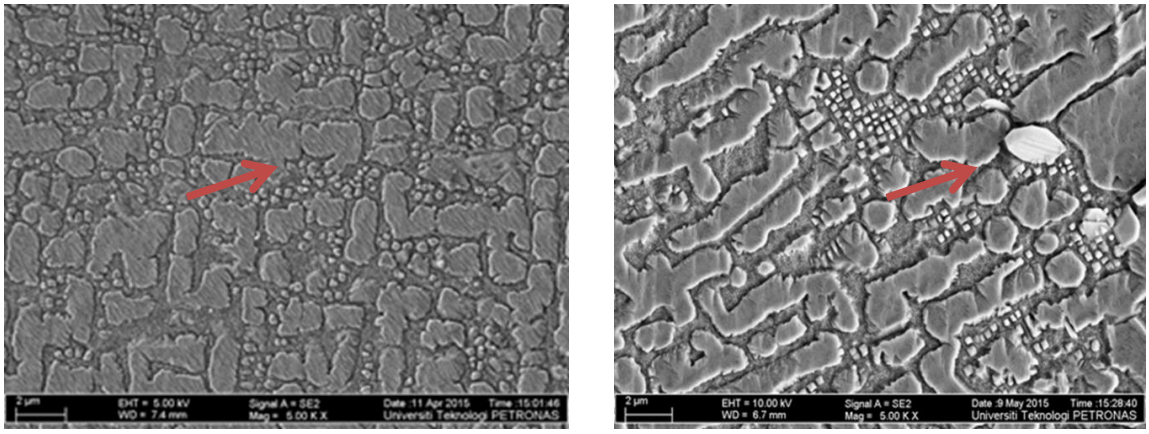

(a) (b)

Figure 4 (a) Microstructure locations B1; (b) Microstructure at location A2.

In addition, Figure 4(a) presents the microstructure for location B1. The cell-like sub-grain sizes reduced at the pressure surface side, as depicted in Figure 4(a) B1; unlike the suction surface side sample specimen A2, which could be due to the coarsened sigma (hardened) phase before shifting to equilibrium phase. More so, the low-density dislocation of the cell-like sub-grain projected discrete development. The formation of bimodal (γ^I) structure at this location demonstrated coarsening of the precipitates. The secondary (γ^I) precipitates appeared less cubical, but instead, had rough edges. Similarly, the primary (γ^I) precipitates were also less cubical in shape, but appeared to be more spherical. In terms of carbides formation, both types of carbides, $M_{23}C_6$ and MC, were successfully detected (not shown) although reduced in population. Finally, the microstructure observation on the middle, lower part of the turbine blade, which is Location A2, is depicted in Figure 4(b). The microstructure showed larger secondary

spheroidal (γ^I) precipitates compared to that for location B1. The population was also higher at location C2. The bimodal structure, nevertheless, still remained similar with that of other locations, except Location A. Moreover, coarsening of both secondary and primary (γ^I) precipitates were observed compared to that in location B1. The structure of the secondary (γ^I) precipitates showed rough edges, while the primary (γ^I) precipitates had distinct cubical structure. In addition, the MC type carbides were also present in the microstructure, as indicated with the arrow. The diffusion-less transformation along the grain boundary was not unclearly detected in the SEM image in Figure 4(a), however, progression of recovery towards grain interior was observed after operation hours and exposure to high temperature. In addition, isolated and discrete carbides had been obvious along the grain boundary. The proportional effects of the growth of these grains with time, unfortunately, remains unpredictable.

CONCLUSIONS

The investigation of a service exposed engine turbine blade have been conducted experimentally to determine the effects of thermal degradation on microstructural changes that occur inside the material and the development of primary MC carbides along the grain boundary. The micrograph images of the blade samples were cut from both suction and pressure side surface locations of the blade to examine the internal changes that took place via SEM imaging. The following depicts the findings drawn from the investigation and some future recommendations within the research area:

1. The changes in microstructural formation of the blade is mainly due to rate of heat, stress exposure, and material elemental composition at different phases;
2. The microstructure of the primary (γ^I) precipitates differs for each location of the engine turbine blade due to various impacts of thermal and stress during operation. The formation of (γ^I) precipitates varies in size and structural shape throughout each location.
3. All locations displayed bimodal distribution of the (γ^I) precipitates, except at the bottom of the blade, location A1. Coarsening effect of the precipitates was mainly observed at the middle section of the blade, locations C1 and B2.
4. A need arises to investigate the phase transition effect on both the primary and secondary MC carbides formation along the grain boundary as this can offer a hint if all locations of the blade failure are consistent with the elemental constituents or if they behaved differently with respect to phase distribution.
5. Analytical tools can be employed to calculate thermal despondences, phase distribution, and the corresponding effect on carbides formation along the grain boundary.

ACKNOWLEDGEMENTS

The authors would like to acknowledge Universiti Teknologi PETRONAS for providing laboratory facilities and MOHE for financial assistance under Fundamental Research Grant Scheme (FRGS).

REFERENCES

[1] Reddy LR. Creep life estimation of gas turbine blade. 2016.

[2] Epishin A, Link T, Klingelhöffer H, Fedelich B, Portella P. Creep damage of single-crystal nickel base superalloys: mechanisms and effect on low cycle fatigue. Materials at high temperatures. 2014.

[3] Dewangan R, Patel J, Dubey J, Sen PK, Bohidar SK. Gas turbines blades-a critical review of failure on first and second stages. International Journal of Mechanical Engineering and Robotics Research. 2015;4:216.

[4] Kovacs S, Beck T, Singheiser L. Influence of mean stresses on fatigue life and damage of a turbine blade steel in the VHCF-regime. International Journal of Fatigue. 2013;49:90-9.

[5] Caron P. High y'solvus new generation nickel-based superalloys for single crystal turbine blade applications. Superalloys 2000. 2000:737-46.

[6] Sajjadi SA, Zebarjad SM, Guthrie R, Isac M. Microstructure evolution of high-performance Ni-base superalloy GTD-111 with heat treatment parameters. Journal of materials processing technology. 2006;175:376-81.

[7] Donachie MJ, Donachie SJ. Superalloys: a technical guide: ASM international; 2002.

[8] Wilson JM, Piya C, Shin YC, Zhao F, Ramani K. Remanufacturing of turbine blades by laser direct deposition with its energy and environmental impact analysis. Journal of Cleaner Production. 2014;80:170-8.

[9] Sujata M, Madan M, Raghavendra K, Venkataswamy M, Bhaumik S. Microstructural study: an aid to determination of failure mechanism in nickel base superalloy blades. Transactions of the Indian Institute of Metals. 2010;63:681-5.

[10] Lvova E, Norsworthy D. Influence of service-induced microstructural changes on the aging kinetics of rejuvenated Ni-based superalloy gas turbine blades. Journal of materials engineering and performance. 2001;10:299-312.

[11] Rybnikov A, Getsov L, Leontiev S. Failure analysis of gas turbine blades. Microscopy and Microanalysis. 2005;11:222-3.

[12] Mikami M, Sawada K, Kobayashi S, Hara T, Kimura K. Microstructural change after long-term creep exposure in high cr steel forgings for ultrasupercritical steam turbine rotors. Advances in Materials Technology for Fossil Power Plants: Proceedings from the Seventh International Conference, October 22-25, 2013 Waikoloa, Hawaii, USA: ASM International; 2014. p. 293.

[13] Tong J, Ding X, Wang M, Yagi K, Zheng Y, Feng Q. Assessment of service induced degradation of microstructure and properties in turbine blades made of GH4037 alloy. Journal of Alloys and Compounds. 2016;657:777-86.

[14] Kuhn F, Zeismann F, Brückner-Foit A, Kadau K, Gravett P. Crack paths in the superalloy IN738 in aged conditions. Engineering Fracture Mechanics. 2013;108:275-84.

[15] Murr L, Martinez E, Pan X, Gaytan S, Castro J, Terrazas C, et al. Microstructures of Rene 142 nickel-based superalloy fabricated by electron beam melting. Acta Materialia. 2013;61:4289-96.